Assessment of an effective quasirelativistic methodology designed to study astatine chemistry in aqueous solution

Julie Champion, Mahamadou Seydou, Andrea Sabatié-Gogova, Eric Renault, Gilles Montavon, Nicolas Galland

Assessment of an effective quasirelativistic methodology designed to study astatine chemistry in aqueous solution†

Julie Champion,[a,b] **Mahamadou Seydou,**[a,b] **Andrea Sabatié-Gogova,**[b] **Eric Renault,**[a] **Gilles Montavon***[b] **and Nicolas Galland***[a]

Abstract. A cost-effective computational methodology designed to study astatine (At) chemistry in aqueous solution has been established. It is based on two-component spin-orbit density functional
10 theory calculations and solvation calculations using the conductor-like polarizable continuum model in conjunction with specific astatine cavities. Theoretical calculations are confronted with experimental data measured for complexation reactions between metallic forms of astatine (At^+ and AtO^+) and inorganic ligands (Cl^-, Br^- and SCN^-). For each reaction, both 1:1 and 1:2 complexes are evidenced. The experimental trends regarding the thermodynamic constants (K) can
15 be reproduced qualitatively and quantitatively. The mean signed error on computed Log K values is -0.4, which corresponds to a mean signed error smaller than 1 kcal mol^{-1} on free energies of reaction. Theoretical investigations show that the reactivity of cationic species of astatine is highly sensitive to spin-orbit coupling and solvent effects. At the moment, the presented computational methodology appears to be the only tool to gain an insight into astatine chemistry at a molecular
20 level.

Introduction

Astatine (At) is the heaviest halogen (element 85), found below iodine in the periodic table of the elements. One of its isotopes, At-211, is a promising candidate as a therapeutic
25 agent in nuclear medicine.[1,2] It is a 100% alpha emitter, with a half life of 7.2 h. Sufficiently high energy X-rays accompany these characteristic alpha emissions, allowing external At-211 distribution imaging.[3] Monitoring the X-ray emissions provides useful concerning the dosimetry, tumor
30 accumulation and normal tissue deposition of At-211-labeled radiopharmaceuticals. Two recent reviews summarize the use of astatine as a radiotherapeutic agent.[4,5] Although much of the chemistry described for halogens is applicable to astatine, the chemical similarities between astatine and its nearest
35 halogen neighbor, iodine, is not always obvious. Indeed, At chemistry in aqueous solution is not well understood. Astatine is one of the most difficult elements to investigate from a chemist's point of view: it is a rare element since there is no stable isotope of astatine (production is with accelerators
40 capable of accelerating alpha particles to high energies), with its longest-lived isotope having a half-life of 8.3 h. It can be considered as an invisible element since all investigations were derived from radiochemical studies at ultra-trace concentrations (typically smaller than 10^{-10} mol/L) and no
45 spectroscopic tools can be used to evaluate astatine chemistry at the molecular level.

From a theoretical point of view, atomic astatine and few small species containing astatine were mainly studied as simple model systems to investigate the reliability of quantum
50 chemistry methods.[6-20] There is currently a growing interest in using relativistic methods for higher-accuracy calculations.

The most accurate approach to incorporate relativity would be to perform four-component (*4c*) calculations based on the exact relativistic Hamiltonian. The straightforward way to
55 construct the relativistic many-electron Hamiltonian is to augment the one-electron Dirac operator with the Coulomb or Breit operator as a two-electron term. Hartree–Fock founded (DHF) and Kohn–Sham (DKS) methods with a four-component Hamiltonian have become familiar[21-23] but they
60 have an intrinsically big computational cost and their use is still limited to small molecules, mostly for benchmarking purposes. While there has been considerable progress in reducing the cost of such calculations,[18,24] the applicability of the four-component theory to large molecular systems is
65 hindered mainly by the comparatively early stage of development of the relevant algorithms and codes.[25] As an alternative approach, several two-component (*2c*) quasirelativistic approximations have been proposed and applied to chemically interesting systems containing heavy
70 elements. Accurate descriptions of relativistic effects could be obtained with the familiar Douglas–Kroll (DK*n*) approach, involving a transformation to the *n*th order of the Dirac Hamiltonian,[13,26] or using the *n*th order regular approximation (ZORA, FORA) of the exact relativistic Hamiltonian.[27,28] For
75 large molecular systems, the most appealing quasirelativistic approach is to switch to relativistic effective core potentials (RECPs) or pseudopotentials (PPs). Approximate calculations based on RECPs or PPs are known to successfully yield results that are very close to the all-electron results without
80 introducing any empirical parameters.[12,16,20,29,30] In this context, several theoretical studies on At, HAt and At_2 species have been conducted, in order to check various relativistic and quasirelativistic computational methods. The theoretical interest in astatine and its compounds is related to the fact that

these species are subject to large relativistic effects, notably spin-orbit (SO) coupling (*cf.* Table S1 in Supplementary Information). High level calculations predict that the SO interactions reduce by one third the astatine's electron affinity (*EA*) and the dissociation energy (D_e) of HAt. In the case of At$_2$, the SO coupling contribution to D_e is greater than the value of the dissociation energy; the vibrational harmonic frequency (ω_e) is also strongly affected (almost 50 % reduction).

Apart from these fundamental studies, no theoretical investigation has been reported concerning one of the few astatine compounds that are experimentally evidenced.[31-39] There is an actual need for a very cost-effective method that enables to study medium size species without neglecting the important SO effects specific to astatine. In this work, we first present experimental results on the complexation properties of the cationic forms of astatine in solution. Recently, At$^+$ and AtO$^+$ species (jointly referred to as At(x)$^+$) have been identified as the major chemical forms of astatine in acidic aqueous solution.[40] Both species were mixed with inorganic ligands, namely Cl$^-$ and Br$^-$, and the complexation constants were measured using a competition method. These findings, and those of a previous study of At(x)$^+$ reactions with SCN$^-$ species,[41] were used in a second step to support an original computational methodology designed to study the astatine chemistry in solution. The theoretical approach has particularly low computational demand because it involves (i) two-component quasirelativistic density functional calculations performed in gas phase, (ii) solvation calculations based on a efficient continuum model, and (iii) all calculations use a relativistic pseudopotential for At atom.

Materials and experimental methodology

Reagents and production of astatine-211

All reagents were of analytical grade or better. The solutions were prepared using Milli-Q water and all experiments were conducted in air-conditioned laboratories. At-211 was produced via the ^{209}Bi(α, 2n)^{211}At nuclear reaction at the cyclotron CEMTHI in Orleans, France. A bismuth target is irradiated for two hours by a 28 MeV alpha external beam.[42] After irradiation of the target, At-211 is isolated using a 'wet' process developed by Alliot *et al.*[43] resulting in a 500 µL solution of 0.1 mol/L NaOH with a specific volume activity close to 1 MBq/mL. The sample's purity was verified and quantified by gamma ray spectroscopy with a high purity germanium (HPGe) detector. The activity of the stock astatine solution was determined using the X-rays from both Po-211 and At-211, as well as the 687.0 keV γ-rays from At-211.[44]

Competition method

At$^+$ was prepared in 0.1 mol/L HClO$_4$ and NaClO$_4$ solution ($pH = 1$ and E ~ 0.6 V *vs*. NHE) and AtO$^+$ with a mixture of 5 10^{-3} mol/L K$_2$Cr$_2$O$_7$, 0.1 mol/L HClO$_4$ and 0.1 mol/L NaClO$_4$ ($pH = 1$ and E ~ 1 V *vs*. NHE).[45-47]The stability constants between inorganic ligands (Cl$^-$, Br$^-$) and cationic species of astatine (At(x)$^+$) were determined using a competition method proposed by Champion *et al.*[41] and

previously used with the SCN$^-$ anion. The method consists in studying the distribution of astatine between aqueous phase and toluene as a function of ligand concentration. The system (5 mL of organic phase and 5 mL of aqueous phase were brought into contact in Pyrex tubes) is first equilibrated before astatine addition. Two hours of shaking were sufficient to achieve distribution equilibrium of At(x)$^+$ between the phases. After phase separation, an aliquot of aqueous and organic phases were withdrawn to derive the distribution coefficient D:

$$D = \frac{V_{\text{org}} \times A_{\text{org}}}{V_{\text{aq}} \times A_{\text{aq}}} \quad (1)$$

where V_{org} and V_{aq} represent the volume of the given phase, and A_{org} and A_{aq} define the isotope's activities in the organic and aqueous phases, respectively. These activities were measured using liquid scintillation counting with a Packard 2550 TR/AB Liquid Scintillation analyzer with the Ultima Gold LLT scintillation liquid.[40] Uncertainties associated with D values were calculated according to the following equation:

$$\sigma_D = D \sqrt{\frac{\sigma_{A_{\text{org}}}^2}{A_{\text{org}}} + \frac{\sigma_{A_{\text{aq}}}^2}{A_{\text{aq}}} + \frac{\sigma_{V_{\text{org}}}^2}{V_{\text{org}}} + \frac{\sigma_{V_{\text{aq}}}^2}{V_{\text{aq}}}} \quad (2)$$

At least three experiments were performed in parallel under the chosen experimental conditions. The average values are given with uncertainties corresponding to a 95% confidence interval.

Determination of the stability constants

Considering the *pKa* values of HCl and HBr,[48] dissolved NaCl and NaBr salts yield in the experimental conditions Cl$^-$ and Br$^-$ species which interact with At(x)$^+$ as follows:

$$\text{At(x)}^+ + m\text{X}^- \underset{}{\overset{\beta_m}{\rightleftharpoons}} \text{At(x)X}_m^{1-m} \quad (3)$$

with X$^-$ corresponding to Cl$^-$ or Br$^-$and At(x)X$_m^{1-m}$ to the complex formed with a 1:m stoichiometry. The stability constant associated to the formation of the complex, β_m, is given by:

$$\beta_m = \frac{(\text{At(x)X}_m^{1-m})}{(\text{At(x)}^+)(\text{X}^-)^m} \quad (4)$$

where the data in parenthesis represent the activities of the species at equilibrium. Without any ligand in solution, astatine distribution D_0 can be expressed by:

$$D_0 = \frac{\overline{\left[At(x)^+\right]}}{\left[At(x)^+\right]} \quad (5)$$

where $\overline{At(x)^+}$ represents astatine species in organic solution and $At(x)^+$ the species in aqueous solution. In the presence of X$^-$ ligands in solution, the distribution of astatine varies and depends on the concentration of the formed complexes:

$$D = \frac{\overline{\left[At(x)^+ \right]}}{\left[At(x)^+ \right] + \sum_{n=1}^{m} \left[At(x)X_n^{1-n} \right]} \qquad (6)$$

Several complexes with 1:n stoichiometry can be present in aqueous solution. Thus, the astatine distribution between aqueous and organic phases can be expressed as a function of the ligand concentration in aqueous solution:

$$D = \frac{D_0}{1 + \sum_n \beta_n \left[X^- \right]^n} \qquad (7)$$

The number and the nature of the formed complexes together with the stability constants were derived by a fitting procedure of titration curves, *i.e.* by analyzing the dependence of D values on X^- concentration. We used the same procedure as described by Champion *et al.*,[41] the modeling involving the CHESS calculation code.[49] All the thermodynamic constants are given for 298.15 K, 1 mol/L standard state and extrapolated at null ionic strength using the Truncated Davies equation.[50]

Computational methodology

SODFT method and basis sets

The application of density functional theory (DFT) appears particularly attractive for heavy-element systems due to the computational expediency and the implicit inclusion of electron correlation effects. However, relativistic effects become as important as electron correlation effects for heavy-elements and should be treated on the same footing. One may distinguish between electron spin-independent (scalar) and spin-dependent effects. The leading spin-dependent effect is the coupling between electron spin and orbital momentum (SO coupling), which in particular for heavy p-elements may be of similar size as scalar relativistic effects. The spin-orbit DFT (SODFT) approach implemented in the NWChem programs package[51] has been successfully used to investigate relativistic effects on molecules containing halogen elements.[30, 52, 53] This approach takes advantage of RECPs and PPs, which replace inner-core electrons and introduce scalar and, optionally, spin-orbit terms into the variational treatment of the one-electron spin-orbit operator, to include SO effects. Furthermore, the non-relativistic formalism operating with orbitals represented by real numbers is extended to a two-component formalism with complex orbitals (spinors). There can be many variations in the form of RECPs and PPs, the present PPs are expressed by the following form:

$$V_{PP}(r) = -\frac{Z_{eff}}{r} + \sum_{ljk} B_{lj}^k \exp\left(-\beta_{lj}^k r^2\right) \mathbf{P}_{lj} \qquad (8)$$

where Z_{eff} is the charge of the inner-core. The sum runs over a Gaussian expansion (index k) of semi-local short-range radial potentials which are different for different orbital angular-momentum quantum numbers l and, for a given l, for the two total one-electron angular-momentum quantum numbers

$j = l \pm 1/2$ ($\mathbf{P}_{lj}$ is the projector onto the complete space of functions with angular symmetry l, j around the core under study). The parameters B_{ljk} and β_{ljk} are adjusted so that V_{PP} in two-component valence-only atomic calculations reproduces, as closely as possible, a set of all-electron reference energies.

We have selected for our calculations the widely used B3LYP[54-57] density functional. Relativistic effects were introduced using the (small-core) scalar or spin-dependent ECP60MDF pseudopotential generated by the Stuttgart/Cologne group for At atom.[12] At first, we opted to the aug-cc-pVDZ-PP (AVDZ) basis set[12] to describe the 25 valence electrons. However, this basis set has been optimized using one-component approach and is not appropriate to describe the SO coupling, in particular on the 5p and 5d inner-shells. As previously demonstrated for other basis sets,[17] adding only few functions with exponents in the range of the inner-shells was sufficient to allow for the splitting of the inner p-shell to an energetically lower lying more compact $p_{1/2}$ and a higher lying less compact $p_{3/2}$ subshell, and similarly that of the d-shell to $d_{3/2}$ and $d_{5/2}$. The resulting basis set is termed mAVDZ (*cf.* Supplementary Information). The performance of the two-component B3LYP calculations in conjunction with ECP60MDF and mAVDZ basis set have been tested on the case of At, HAt and At_2 reference species. Calculated spectroscopic constants are presented in Table 1 and compared to the results of high level calculations. We define the spin-orbit effects (ΔSO) as the difference between scalar and quasirelativistic values calculated B3LYP/mAVDZ level of theory. Considering all the studied properties (and the

Table 1 Spectroscopic constants of At, HAt and At_2 species calculated at B3LYP/mAVDZ level of theory

		Reference values[a]	B3LYP/mAVDZ
At	*IE (eV)*	9.21	9.37
	ΔSO	*-0.82*	*-0.74*
	EA (eV)	2.30	2.43
	ΔSO	*-0.80*	*-0.76*
HAt[b]	D_e *(eV)*	2.36	2.37
	ΔSO	*-0.71*	*-0.70*
	ω_e *(cm^{-1})*	1962	1945
	ΔSO	*-194*	*-151*
	R_e *(Å)*	1.74	1.75
	ΔSO	*0.03*	*0.03*
At_2	D_e *(eV)*	0.63	0.62
	ΔSO	*-1.07*	*-0.98*
	ω_e *(cm^{-1})*	107	104
	ΔSO	*-44*	*-45*
	R_e *(Å)*	3.06	3.09
	ΔSO	*0.17*	*0.17*

[a] Average values calculated from results of high level calculations reported in literature (Ref. 8, 9, 13, 14, 16, 52, 61, 62). [b] aug-cc-pVDZ basis set was used for H atom (Ref. 58, 59).

magnitude of the SO effects) for At, HAt and At$_2$ species, the overall B3LYP/mAVDZ results is in remarkable agreement with the reference values. The agreement is especially good for the diatomic species: in the case of At$_2$, the computed D_e, ω_e and R_e values are, respectively, 0.62 eV, 104 cm^{-1} and 3.09 Å while the results of reference high level calculations are centered around 0.63 eV, 107 cm^{-1} and 3.06 Å. This is very encouraging in view of building a cost-effective methodology to study astatine chemistry.

In the following study of At(x)$^+$, X$^-$ and At(x)X$_m^{1-m}$ (X = Cl, Br and SCN) species, the mAVDZ basis set was used in conjunction with the aug-cc-pVDZ-PP basis set for Br atom[12] and the aug-cc-pVDZ basis sets for Cl, C, O, S and N atoms.[58-60] The bromine (1s-2p) inner-cores were replaced by the energy-consistent ECP10MDF pseudopotential.[12] Despite the fact that relatively small basis sets were selected, our computational methodology makes use of error cancellation approaches and high-quality results are obtained (see section Computation of equilibrium constants for ligand exchange reactions). Gas phase free energies of At(x)$^+$, X$^-$ and At(x)X$_m^{1-m}$ species were estimated at $T = 298.15$ K and $p = 1$ atm through the computation of their energy and geometry by means of the gradient technique. Harmonic vibrational frequencies were evaluated using either analytical second derivative (scalar relativistic level of theory) or by two-sided finite differences of analytical gradients (quasirelativistic level of theory). In the case of At(x)X$_m^{1-m}$ species that exhibit several isomers, their Gibbs free energies have been evaluated using a Boltzmann distribution according to the relation:

$$G_{\{A\}}^{\circ} = -RT \ln \sum_{i \in \{A\}} e^{-G_i^{\circ}/RT} \tag{9}$$

where {A} emphasizes calculation over the population of all isomers of A.

Solvation and cavity models

Gibbs free energies of aqueous solvation were computed for all species using the polarizable continuum model (PCM) implemented in the Gaussian 03 program package.[63] While this model does not account for SO effects, the (larger) contribution of the solute geometry relaxation to the solvation free energies could be evaluated by geometry optimization within the solvent model at scalar relativistic level of theory. We selected the conductor-like formulation, CPCM,[64, 65] since this model, when used in conjunction with the UAHF and UAKS cavity models, yields accurate solvation free energies at a very low computational cost.[66] UAHF and UAKS cavities were built up using the united atom topological model applied on optimized atomic spheres.[63, 67] The spheres' radii depend on the nature of the element and its molecular environment (basically hybridization, formal charge and first neighbor inductive effect). However, at present no parameters for astatine are included in these cavity models. Recently, we proposed to use for At a basic radius (R^0) of 2.41 Å coherent with the rest of the radii included in the UAHF (and UAKS) model.[40] Because At(x)$^+$ and At(x)X$_m^{1-m}$ species display

structures where the At atom bears a positive charge, this leads us to define as well a charge factor (γ_q) for astatine as described in UAHF and UAKS models. We propose to estimate γ_q by use of the experimental value of the At$^+$/At$^-$ standard redox potential: $E^{\circ} = 0.36 \pm 0.01$ V (vs. NHE).[40] As it will be explained using the thermodynamic cycle displayed in Scheme 1, the r_{At^+} radius is the only parameter that needed to be adjusted in order to reproduce the E° value.

The Gibbs free energies of the At$^+$ reduction reaction, ΔG_s^*, is related to the absolute standard reduction potential via the Nernst equation:
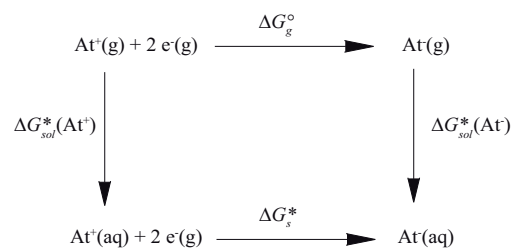
$$E^{\circ} = -\frac{\Delta G_s^*}{nF} \tag{10}$$

where n is the number of electrons transferred ($n = 2$ in this case) and F is the Faraday constant (96485 C/mol). In addition, ΔG_s^* can be calculated from the free energy of the gas-phase reaction, ΔG_g°, according to the relation:

$$\Delta G_s^* = \Delta G_g^{\circ} + \Delta G_{sol}^*(At^-) - \Delta G_{sol}^*(At^+) \tag{11}$$

where $\Delta G_{sol}^*(At^-)$ and $\Delta G_{sol}^*(At^+)$ are respectively the solvation free energies of At$^-$ and At$^+$ in water. ΔG_g° is estimated using the electron affinity ($EA = 2.30$ eV) and ionization energy ($IE = 9.21$ eV) obtained from reference high level calculations done on astatine (see Table 1). For the free electron, we have followed the electron convention based on Boltzmann statistics (the absolute value of the standard reduction potential of NHE is 4.28 V in this convention).[68] $\Delta G_{sol}^*(At^-)$ and $\Delta G_{sol}^*(At^+)$ are determined by CPCM calculations at scalar-relativistic HF/mAVDZ and B3LYP/mAVDZ levels of theory. These quantities rely on r_{At^-} and r_{At^+} radii, respectively. The r_{At^-} value is not free, it must be 0.3 Å shorter than the At basic radius in UAHF and UAKS cavity models (therefore, $r_{At^-} = 2.11$ Å). ΔG_g° and $\Delta G_{sol}^*(At^-)$ values are then fixed. The r_{At^+} radius was adjusted in order to yield a value for $\Delta G_{sol}^*(At^+)$ that allows us to reproduce, using relation (10) and (11), the experimental value of E°. The best agreement is obtained with $r_{At^+} = 1.54$ Å, corresponding to $\gamma_q = -0.87$ Å for an astatine atom with a positive charge. Note that in the CPCM model, the solvation free energy is partitioned in different terms. The most important one is the electrostatic term. Some other terms are usually negligible[66] while the dispersion and repulsion terms are unavailable for astatine. Furthermore, the sum of non-electrostatic terms is generally weak with respect to the electrostatic term, especially for charged species, due to the

Scheme 1

Equilibrium	At⁺			AtO⁺		
	Cl⁻	Br⁻	SCN⁻	Cl⁻	Br⁻	SCN⁻
$At(x)^+ + X^- \underset{}{\overset{\text{Log }\beta_1}{\rightleftharpoons}} At(x)X$	1.9 ± 0.2	3.0 ± 0.2	3.8 ± 0.2	2.5 ± 0.2	2.7 ± 0.2	2.8 ± 0.2
$At(x)^+ + 2X^- \underset{}{\overset{\text{Log }\beta_2}{\rightleftharpoons}} At(x)X_2^-$	2.3 ± 0.1	4.1 ± 0.3	5.9 ± 0.3	3.0 ± 0.3	5.0 ± 0.2	5.3 ± 0.2
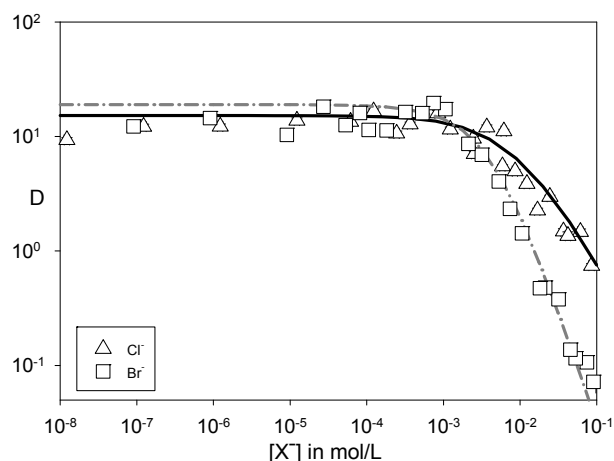
Fig. 1 AtO⁺ interaction with Cl⁻ and Br⁻ in a biphasic aqueous-toluene system. The distribution coefficient (*D*) is plotted as a function of ligand concentration: Cl⁻ (triangles) and Br⁻ (squares). The curves correspond to modeling performed with CHESS using the parameters given in Table 2 (grey dashed line for AtO⁺/Cl⁻ system and black solid line for AtO⁺/Br⁻ system).
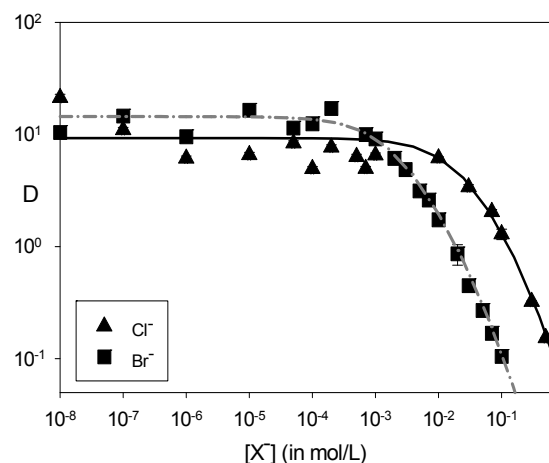

Fig. 2 At⁺ interaction with Cl⁻ and Br⁻ in a biphasic aqueous-toluene system. The distribution coefficient (*D*) is plotted as a function of ligand concentration: Cl⁻ (triangles) and Br⁻ (squares). The curves correspond to modeling performed with CHESS using the parameters given in Table 2 (grey dashed line for AtO⁺/Cl⁻ system and black solid line for AtO⁺/Br⁻ system).

cancellation of different contributions.[69] This could be exemplified on the case of the studied inorganic ligands: Cl⁻, Br⁻ and SCN⁻. The sum of non-electrostatic terms contributes around 1% of the total solvation free energy. Hence, for all studied species we only retained the electrostatic term in CPCM computations and we expect that some error cancellations will occur.

For $At(x)^+$, X^- and $At(x)X_m^{1-m}$ species, the solvation free energies were first determined by CPCM-UAKS calculations at the B3LYP/mAVDZ level of theory (scalar ECP10MDF and ECP60MDF pseudopotentials were used for Br and At atoms, respectively). Geometries of the molecular species were optimized in gas-phase and in presence of the solvent. A second scheme was also used to determine solvation free energies based on CPCM-UAHF calculations. In this case, only single point HF/mAVDZ energy computations were performed on previously optimized geometries at the B3LYP/mAVDZ level of theory and in presence of the solvent.

Results and discussion

Experimental results

Fig. 1 displays the distribution of the AtO⁺ species in a biphasic aqueous–toluene solution as a function of Cl⁻ and Br⁻ ligand concentrations. The grey dashed and black solid lines are based on modeling using the parameters (complexation constants) gathered in Table 2. Ligand concentrations lower than 10^{-5} mol/L do not affect astatine's distribution coefficients *D*. The decrease of *D* value for $[X^-] > 10^{-5}$ mol/L is an evidence of AtO⁺ complexation by X⁻ in aqueous solution. Analyzing the dependence of *D* values on X⁻ concentration yields the number and speciation of the species formed as well as their stability constants.[41] The simulation and associated curves of Fig. 1 demonstrate that the interaction of AtO⁺ with Cl⁻ and Br⁻ involve the formation of both 1:1 and 1:2 complexes. The thermodynamic constants, β_1 and β_2, describing this interaction are reported in Table 2. The interaction constants between AtO⁺ and Br⁻ agree with the published data of Dreyer *et al.*[70] obtained by electromobility measurements. They found a value of Log K_2 equal to 2.4 for the reaction:

$$AtOBr + Br^- \underset{}{\overset{K_2}{\rightleftharpoons}} AtOBr_2^- \qquad (12)$$
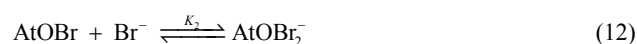
which is equal, within experimental errors, to the one calculated from β_1 and β_2, *i.e.* Log $K_2 = 2.3 \pm 0.4$.
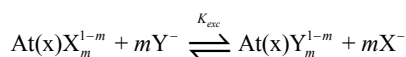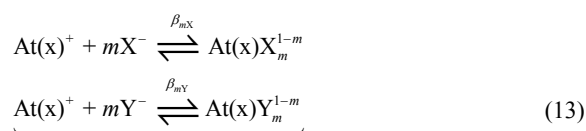
Table 2 also includes the thermodynamic constants deduced for the interaction of the At⁺ species with Cl⁻ and Br⁻. Experimental data and simulation curves are displayed in Fig. 2. Similar results are obtained: experimental results and modeling agree when we consider the formation of a mixture of AtBr and $AtBr_2^-$ species. Thus, interactions between the cationic $At(x)^+$ species with small inorganic ligands result in the formation of two complexes with 1:1 and 1:2

stoichiometries. This phenomena was previously observed with thiocyanate ligand (Table 2).[41] From the gathered results in Table 2, it appears that the efficiency of the $At(x)^+$ interaction with the inorganic ligands increases in the order $Cl^- < Br^- < SCN^-$, regardless of the considered stoichiometry. According to the HSAB theory (Hard and Soft Acids and Bases), the astatine metallic species can be considered as soft acids.

Quantum calculations

Computation of equilibrium constants for ligand exchange reactions

As it could be expected, the attempt to compute equilibrium constants for complexation reactions as described by equation (3) between $At(x)^+$ and ligands (Cl^-, Br^- or SCN^-) were unsuccessful. The theoretical predictions appear randomly qualitatively and/or quantitatively inaccurate for the complexation reaction studied (*cf.* Table S2 in Supplementary Information). A more promising alternative approach for studying astatine chemistry is to consider reactions that correspond to an exchange of ligands (X^- and Y^-) as follows:

$$At(x)^+ + mX^- \overset{\beta_{mX}}{\rightleftharpoons} At(x)X_m^{1-m}$$

$$\underbrace{At(x)^+ + mY^- \overset{\beta_{mY}}{\rightleftharpoons} At(x)Y_m^{1-m}}$$ (13)

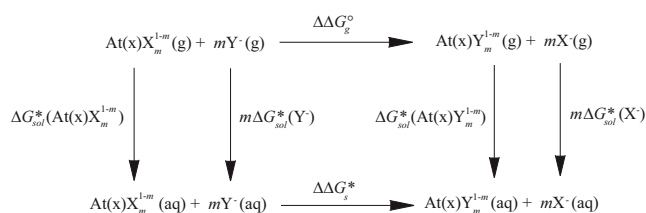$$At(x)X_m^{1-m} + mY^- \overset{K_{exc}}{\rightleftharpoons} At(x)Y_m^{1-m} + mX^-$$

The equilibrium constant of the exchange reactions can be obtained from the experimental constants of complexation reactions: $K_{exc} = \beta_{mY} / \beta_{mX}$. In addition, K_{exc} can be calculated from the computed standard free energy change of reaction (13) in solution, $\Delta\Delta G_s^*$. As Scheme 2 shows, $\Delta\Delta G_s^*$ can be calculated from its components by introducing a thermodynamic cycle:

$$\Delta\Delta G_s^* = \Delta\Delta G_g^\circ + \Delta G_{sol}^*\left(At(x)Y_m^{1-m}\right) + m\Delta G_{sol}^*\left(X^-\right)$$
$$- \Delta G_{sol}^*\left(At(x)X_m^{1-m}\right) - m\Delta G_{sol}^*\left(Y^-\right)$$ (14)

where $\Delta\Delta G_g^\circ$ is the change of free energy in the gas-phase; $\Delta G_{sol}^*\left(At(x)X_m^{1-m}\right)$, $\Delta G_{sol}^*\left(At(x)Y_m^{1-m}\right)$, $\Delta G_{sol}^*\left(X^-\right)$ and $\Delta G_{sol}^*\left(Y^-\right)$ are, respectively, the solvation free energies of $At(x)X_m^{1-m}$, $At(x)Y_m^{1-m}$, X^- and Y^- species in water. Therefore the prediction of $\Delta\Delta G_s^*$ could benefit from:

1 bond-by-bond errors in electron correlation/relativistic contributions which partially cancel in the computed gas-phase free energy, $\Delta\Delta G_g^\circ$.

At(x)X$_m^{1-m}$(g) + mY$^-$(g) $\xrightarrow{\Delta\Delta G_g^\circ}$ At(x)Y$_m^{1-m}$(g) + mX$^-$(g)

$\Delta G_{sol}^*(At(x)X_m^{1-m})$ $m\Delta G_{sol}^*(Y^-)$ $\Delta G_{sol}^*(At(x)Y_m^{1-m})$ $m\Delta G_{sol}^*(X^-)$

At(x)X$_m^{1-m}$(aq) + mY$^-$(aq) $\xrightarrow{\Delta\Delta G_s^*}$ At(x)Y$_m^{1-m}$(aq) + mX$^-$(aq)

Scheme 2

2 cancellations of systematic errors (including the neglect of non-electrostatic and SO contributions) associated with the calculations of solvation free energies, ΔG_{sol}^*, for ionic species and for neutral species.

More similar are the X^- and Y^- ligands, more the cancellations of errors will act and better will be the resulting prediction.

Table 3 reports experimental and calculated values of Log K_{exc} for eight reactions corresponding to an exchange of ligands (X^-, $Y^- = Cl^-$, Br^- and SCN^-, $m = 1, 2$). First are given the Log K_{exc} values that correspond to exchange reactions in gas phase, $\Delta\Delta G_g^\circ$ being computed at the scalar-relativistic B3LYP/mAVDZ level of theory. The effects of the solvent on these reactions and Log K_{exc} values are next introduced through CPCM-UAHF computations of solvation free energies. The final results include the contribution of SO coupling, computed at quasirelativistic B3LYP/mAVDZ level of theory, in the $\Delta\Delta G_g^\circ$ component. This separation of contributions allows for the demonstration of the following:

1 the astatine affinity with the studied ligands is totally reversed between the gas phase and the aqueous phase. For example, the trend predicted in gas phase for the formation of 1:1 complexes with At^+ is $SCN^- < Br^- < Cl^-$ while the observed trend in water is $Cl^- < Br^- < SCN^-$.

2 solvent effects hardly modify the Log K_{exc} values and almost always allow us to recover experimental trends: in the case of $AtBr_2^- + 2SCN^-$ reaction, the reaction direction get better and the computed Log K_{exc} value changes from -10.4 to 1.0 (which is close to the experimental value of 1.8 ± 0.6).

3 besides the inclusion of spin-independent relativistic effects, the contribution of SO coupling must be taken into account during the evaluation of $\Delta\Delta G_g^\circ$ in order to reach a quantitative agreement with experimental Log K_{exc} values.

Table 3 Computed values of Log K_{exc} based on B3LYP/mAVDZ and CPCM-UAHF calculations

	AtX + Y$^-$ $\rightleftharpoons$ AtY + X$^-$		AtOX + Y$^-$ $\rightleftharpoons$ AtOY + X$^-$	
Log K_{exc} X$^-$/Y$^-$	Cl$^-$/Br$^-$	Br$^-$/SCN$^-$	Cl$^-$/Br$^-$	Br$^-$/SCN$^-$
Gas phase[a]	-0.5	-7.4	-1.3	12.5
Aqueous phase[b]	3.2	1.3	0.9	-0.2
Inclu. SO[c]	2.0	1.0	0.3	-0.1
Experiment	1.1 ± 0.4	0.8 ± 0.4	0.2 ± 0.4	0.1 ± 0.4

	AtX$_2^-$ + 2Y$^-$ $\rightleftharpoons$ AtY$_2^-$ + 2X$^-$		AtOX$_2^-$ + 2Y$^-$ $\rightleftharpoons$ AtOY$_2^-$ + 2X$^-$	
Log K_{exc} X$^-$/Y$^-$	Cl$^-$/Br$^-$	Br$^-$/SCN$^-$	Cl$^-$/Br$^-$	Br$^-$/SCN$^-$
Gas phase[a]	-3.7	-10.4	-4.6	-13.7
Aqueous phase[b]	2.2	1.0	1.1	-1.4
Inclu. SO[c]	1.7	1.1	0.8	-2.0
Experiment	1.8 ± 0.4	1.8 ± 0.6	2.0 ± 0.5	0.3 ± 0.4

[a] Exchange reactions in gas phase; $\Delta\Delta G_g^\circ$ values based on scalar-relativistic B3LYP/mAVDZ calculations. [b] Exchange reactions in water; solvation free energies based on CPCM-UAHF calculations. [c] Exchange reactions in water; $\Delta\Delta G_g^\circ$ values based on quasirelativistic B3LYP/mAVDZ calculations.

The best examples are AtCl + Br⁻ and AtOCl + Br⁻ reactions for which Log K_{exc} values are improved by 1.2 and 0.6, respectively.

Finally, we observe that only quasirelativistic B3LYP/mAVDZ calculations coupled with CPCM-UAHF solvation calculations can reproduce satisfactorily the equilibrium constants of the exchange reaction. For the eight reactions studied, the mean unsigned error (MUE, calculated as the unsigned differences between the Log K_{exc} values obtained using the experimental stability constants gathered in Table 2 and the Log K_{exc} values obtained using quantum computations) on Log K_{exc} values is 0.7, which corresponds to a MUE smaller than 1 kcal mol⁻¹ on $\Delta\Delta G_s^*$, and the mean signed error (MSE, calculated as the differences between the Log K_{exc} values obtained using the experimental stability constants gathered in Table 2 and the Log K_{exc} values obtained using quantum computations) on Log K_{exc} values is -0.4. Two results need nevertheless more attention. In the Br⁻/SCN⁻ exchange reactions with AtO⁺ and for both the 1:1 and 1:2 complexes, the exchange reactions seem predicted in the wrong direction (AtO⁺ will have a better affinity for Br⁻ than for SCN⁻). The Log K_{exc} values obtained from experiment, 0.1 and 0.3 respectively, show very balanced reactions between reactants ($AtBr_m^{1-m} + mSCN^-$) and products ($AtSCN_m^{1-m} + mBr^-$). Moreover, in the case of the exchange between the 1:1 complexes, the computed value of -0.1 is within the experimental Log K_{exc} uncertainty range, [-0.3;+0.5]. The exchange reaction between the 1:2 complexes contrasts with the previous one, making the disagreement between experiment and theory obvious: experimental and computed Log K_{exc} values differ by 2.3 (which contributes by 32% and 64% to the MUE and MSE on Log K_{exc}, respectively). In this case, the theoretical predictions are likely to suffer from the deficiencies of the solvation models used.

Solvent and spin-orbit effects

The Log K_{exc} values predicted by quasirelativistic B3LYP/mAVDZ calculations coupled with CPCM-UAKS solvation calculations (*cf.* Table S3 in Supplementary Information) are in lesser agreement with the experiment: the MUE and MSE on Log K_{exc} values increase to 1.5 and -1.1, respectively. This observation highlights the importance of the solvent model and CPCM-UAHF calcultations appear recommend for the computation of the solvation free energies of astatine species in water.

The AtOBr + SCN⁻ reaction illustrates well the influence of solvent and SO effects on astatine chemistry. Among the possible products, the most important ones are NCSAtO, SCNAtO, NCSOAt and SCNOAt as displayed in Fig. 3. Table 4 reports the population of each species evaluated using a Boltzmann distribution according to the relation 15:
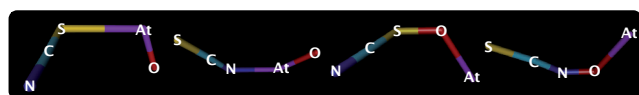

Fig. 3 Molecular structures of NCSAtO, SCNAtO, NCSOAt and SCNOAt species (from left to right).

Table 4 Relative Boltzmann population (%) of NCSAtO, SCNAtO, NCSOAt and SCNOAt species computed at different levels of theory

Species	NCSAtO	SCNAtO	NCSOAt	SCNOAt
Gas phase[a]	0	0	100	0
Aqueous phase[b]	75	25	0	0
Inclu. SO[c]	9	91	0	0

[a] Based on gas phase free energies computed at the scalar-relativistic B3LYP/mAVDZ level of theory. [b] Based on free energies corrected from solvent effects contribution (CPCM-UAHF calculations). [c] Gas phase free energies include SO effects computed at the quasirelativistic B3LYP/mAVDZ level of theory.

$$p_i = \frac{e^{-G_i/RT}}{\sum_{j=1}^{4} e^{-G_j/RT}} \tag{15}$$

The NCSOAt species is predicted by scalar-relativistic B3LYP/mAVDZ calculations as the predominant isomer in gas phase, its relative population approaching 100%. Solvent effects on the distribution of the four isomers is huge. If the solvation free energies are estimated from CPCM-UAHF calculations, the NCSOAt species vanishes while the SCNAtO and NCSAtO isomers rise to a population of 25% and 75%, respectively. The final results include the contribution of SO coupling, computed at the quasirelativistic B3LYP/mAVDZ level of theory, in the estimation of the free energy of the four isomers. In conjunction with CPCM-UAHF calculations, the inclusion of SO effects reverses the relative populations of SCNAtO and NCSAtO species: astatine appears to have a better affinity for the N atom than for the S atom. The predominant species is then SCNAtO, with a predicted relative population of 91%, while NCSAtO represents 9% of the isomers distribution (the remaining two species are negligible). These results show how the solvent and the relativistic effects due to spin-orbit coupling strongly influence the elemental astatine chemistry at a molecular level.

Conclusions

The stability constants in water between inorganic ligands (Cl⁻, Br⁻ and SCN⁻) and At⁺ and AtO⁺ species were measured using a competition method. For each reaction, both 1:1 and 1:2 complexes are evidenced. The two astatine forms exhibit a better affinity for SCN⁻ than Br⁻, with Cl⁻ being the weakest ligand. The experimental trends regarding the thermodynamic constants can be reproduced qualitatively and quantitatively using an especially cost-effective computational methodology. Besides the treatment of the scalar relativistic effects, the leading spin-dependent effect, *i.e.* the spin-orbit coupling, must be taken into account at least within the one-electron approximation. The presented methodology is based on (i) two-component B3LYP calculations using a small-core pseudopotential together with an enhanced valence double zeta basis set for At, and (ii) solvation calculations using the CPCM continuum model in conjunction with specific astatine cavities. The MUE and MSE on computed Log K values are 0.7 and -0.4, respectively. The obtained agreement validates

the theoretical calculations and strengthens the reliability of the experimental methodology. Theoretical investigations have shown that the astatine chemistry is largely modified by spin-orbit coupling and solvent effects. We believe that the presented computational methodology is accurate enough to gain an insight into the astatine reactions at a molecular level.

Acknowledgment

References

ᵃ Laboratoire CEISAM, UMR CNRS 6230, Université de Nantes, 2 Rue de la Houssinière, BP 92208, 44322 Nantes Cedex 3, France. Fax: +33 251 125 567; Tel: +33 251 125 571; E-mail: nicolas.galland@univ-nantes.fr

ᵇ Laboratoire SUBATECH, IN2P3/CNRS/EMN Nantes/Université de Nantes, 4 rue A. Kastler, BP 20722, 44307 Nantes Cedex 03, France. Fax: +33 251 858 479; Tel: +33 251 858 420; E-mail: montavon@subatech.in2p3.fr

† Electronic Supplementary Information (ESI) available: Calculated spectroscopic constants of At, HAt and At$_2$ species from literature (Table S1); computed equilibrium constants for three complexation reactions (Table S2); computed exchange equilibrium constants based on CPCM-UAKS solvation calculations (Table S3); the modified aug-cc-pVDZ-PP astatine basis set used in this work. See DOI: 10.1039/b000000x/

1. M. R. McDevitt, G. Sgouros, R. D. Finn, J. L. Humm, J. G. Jurcic, S. M. Larson and D. A. Scheinberg, *Eur. J. Nucl. Med.*, 1998, **25**, 1341-1351.
2. M. R. Zalutsky, D. A. Reardon, G. Akabani, R. E. Coleman, A. H. Friedman, H. S. Friedman, R. E. McLendon, T. Z. Wong and D. D. Bigner, *J. Nucl. Med.*, 2008, **49**, 30-38.
3. T. G. Turkington, M. R. Zalutsky, R. J. Jaszczak, P. K. Garg, G. Vaidyanathan and R. E. Coleman, *Phys. Med. Biol.*, 1993, **38**, 1121-1130.
4. D. S. Wilbur, *Curr. Radiopharm.*, 2008, **1**, 144-176.
5. G. Vaidyanathan and M. R. Zalutsky, *Curr. Radiopharm.*, 2008, **1**, 177-196.
6. W. Kuechle, M. Dolg, H. Stoll and H. Preuss, *Mol. Phys.*, 1991, **74**, 1245-1263.
7. L. Visscher, J. Styszynski and W. C. Nieuwpoort, *J. Chem. Phys.*, 1996, **105**, 1987-1994.
8. L. Visscher and K. G. Dyall, *J. Chem. Phys.*, 1996, **104**, 9040-9046.
9. Y.-K. Han, C. Bae and Y. S. Lee, *J. Chem. Phys.*, 1999, **110**, 8969-8975.
10. T. Fleig and A. J. Sadlej, *Phys. Rev. A: Gen. Phys.*, 2002, **65**, 032506.
11. P. Norman, B. Schimmelpfennig, K. Ruud, H. J. A. Jensen and H. Agren, *J. Chem. Phys.*, 2002, **116**, 6914-6923.
12. K. A. Peterson, D. Figgen, E. Goll, H. Stoll and M. Dolg, *J. Chem. Phys.*, 2003, **119**, 11113-11123.
13. T. Nakajima and K. Hirao, *J. Chem. Phys.*, 2003, **119**, 4105-4111.
14. B. O. Roos, R. Lindh, P.-A. Malmqvist, V. Veryazov and P.-O. Widmark, *J. Phys. Chem. A*, 2004, **108**, 2851-2858.
15. E. Fromager, L. Maron, C. Teichteil, J.-L. Heully, K. Faegri and K. Dyall, *J. Chem. Phys.*, 2004, **121**, 8687-8698.
16. A. Mitin, V. and C. van Wullen, *J. Chem. Phys.*, 2006, **124**, 64305.
17. M. K. Armbruster, W. Klopper and F. Weigend, *Phys. Chem. Chem. Phys.*, 2006, **8**, 4862-4865.
18. D. Peng, W. Liu, Y. Xiao and L. Cheng, *J. Chem. Phys.*, 2007, **127**, 104106/104101-104106/104115.
19. M. K. Armbruster, F. Weigend, C. van Wuellen and W. Klopper, *Phys. Chem. Chem. Phys.*, 2008, **10**, 1748-1756.
20. F. Wang, J. Gauss and C. van Wuellen, *J. Chem. Phys.*, 2008, **129**, 064113/064111-064113/064117.
21. L. Visscher, O. Visser, P. J. C. Aerts, H. Merenga and W. C. Nieuwpoort, *Comput. Phys. Commun.*, 1994, **81**, 120-144.
22. M. Abe, H. Iikura, M. Kamiya, T. Nakajima, S. Yanagisawa and T. Yanai, *REL4D*, (2004) University of Tokyo, Tokyo, Japan.
23. L. Visscher, H. J. A. Jensen, T. Saue, R. Bast, S. Dubillard, K. G. Dyall, U. Ekström, E. Eliav, T. Fleig, A. S. P. Gomes, T. U. Helgaker, J. Henriksson, M. Iliaš, C. R. Jacob, S. Knecht, P. Norman, J. Olsen, M. Pernpointner, K. Ruud, P. Sałek and J. Sikkema, *DIRAC*, (2008) see http://dirac.chem.sdu.dk.
24. M. Ilias and T. Saue, *J. Chem. Phys.*, 2007, **126**, 064102/064101-064102/064109.
25. L. Belpassi, F. Tarantelli, A. Sgamellotti and H. M. Quiney, *Phys. Rev. B*, 2008, **77**, 233403/233401-233403/233404.
26. C. L. Collins, K. G. Dyall and H. F. Schaefer, III, *J. Chem. Phys.*, 1995, **102**, 2024-2031.
27. E. van Lenthe, E. J. Baerends and J. G. Snijders, *J. Chem. Phys.*, 1994, **101**, 9783-9792.
28. M. Filatov and D. Cremer, *Mol. Phys.*, 2003, **101**, 2295-2302.
29. W. C. Ermler, R. B. Ross and P. A. Christiansen, *Adv. Quantum Chem.*, 1988, **19**, 139-182.
30. H. S. Lee, W. K. Cho, Y. J. Choi and Y. S. Lee, *Chem. Phys.*, 2005, **311**, 121-127.
31. E. H. Appelman, *J. Phys. Chem.*, 1961, **65**, 325-331.
32. E. H. Appelman, E. N. Sloth and M. H. Studier, *Inorg. Chem.*, 1966, **5**, 766-769.
33. Y. V. Norseev and V. A. Khalkin, *J. Inorg. Nucl. Chem.*, 1968, **30**, 3239-3243.
34. T. Do Kim, I. V. Dudova and V. A. Khalkin, *Radiokhimiya*, 1973, **15**, 548-553.
35. N. A. Golovkov, I. I. Gromova, M. Janicki, Y. V. Norseev, V. G. Sandukovskii and L. Vasaros, *Radiochem. Radioanal. Lett.*, 1980, **44**, 67-78.
36. R. Dreyer, I. Dreyer, F. Roesch and G. J. Beyer, *Radiochem. Radioanal. Lett.*, 1982, **54**, 165-175.
37. R. Dreyer, I. Dreyer, M. Pfeiffer and F. Roesch, *Radiochem. Radioanal. Lett.*, 1983, **55**, 207-213.
38. R. Dreyer, I. Dreyer, S. Fischer, H. Hartmann and F. Roesch, *J. Radioanal. Nucl. Chem.*, 1985, **96**, 333-341.
39. S. Fischer, R. Dreyer and S. Albrecht, *J. Radioanal. Nucl. Chem.*, 1987, **117**, 275-283.
40. J. Champion, C. Alliot, E. Renault, B. M. Mokili, M. Cherel, N. Galland and G. Montavon, *J. Phys. Chem. A*, 2010, **114**, 576-582.
41. J. Champion, C. Alliot, S. Huclier, D. Deniaud, Z. Asfari and G. Montavon, *Inorg. Chim. Acta*, 2009, **362**, 2654-2661.
42. G. Henriksen, S. Messelt, E. Olsen and R. H. Larsen, *Appl. Radiat. Isot.*, 2001, **54**, 839-844.
43. C. Alliot, M. Cherel, J. Barbet, T. Sauvage and G. Montavon, *Radiochim. Acta*, 2009, **97**, 161-165.
44. F. Groppi, M. L. Bonardi, C. Birattari, E. Menapace, K. Abbas, U. Holzwarth, A. Alfarano, S. Morzenti, C. Zona and Z. B. Alfassi, *Appl. Radiat. Isot.*, 2005, **63**, 621-631.
45. F.-C. Wang, Y. V. Norseev, V. A. Khalkin and T.-N. Chao, *Radiokhimiya*, 1963, **5**, 351-355.
46. K. Berei and L. Vasaros, *Astatine Compounds*, 8th edn., Springer-Verlag, Berlin, 1985.
47. T. K. Hung, M. Milanov, F. Rosch and V. A. Khalkin, *Radiochim. Acta*, 1989, **47**, 105-108.
48. R. J. P. Williams and J. J. R. Frausto da Silva, *The Natural Selection of the Chemical Elements: The Environment and Life's Chemistry*, Oxford University Press, Oxford, 1996.

49. J. van der Lee and L. De Windt, *J. Contam. Hydrol.*, 2001, **47**, 265-282.

50. B. J. Colston and V. J. Robinson, *J. Environ. Radioact.*, 1995, **29**, 121-136.

51. T. P. Straatsma, E. Aprà, T. L. Windus, E. J. Bylaska, W. de Jong, S. Hirata, M. Valiev, M. Hackler, L. Pollack, R. Harrison, M. Dupuis, D. M. A. Smith, J. Nieplocha, T. V., M. Krishnan, A. A. Auer, E. Brown, G. Cisneros, G. Fann, H. Früchtl, J. Garza, K. Hirao, R. Kendall, J. Nichols, K. Tsemekhman, K. Wolinski, J. Anchell, D. Bernholdt, P. Borowski, T. Clark, D. Clerc, H. Dachsel, M. Deegan, K. Dyall, D. Elwood, E. Glendening, M. Gutowski, A. Hess, J. Jaffe, B. Johnson, J. Ju, R. Kobayashi, R. Kutteh, Z. Lin, R. Littlefield, X. Long, B. Meng, T. Nakajima, S. Niu, M. Rosing, G. Sandrone, M. Stave, H. Taylor, G. Thomas, J. van Lenthe, A. Wong and Z. Zhang, *NWChem, A Computational Chemistry Package for Parallel Computers, Version 5.1.1*, (2008) Pacific Northwest National Laboratory, Richland, Washington 99352-0999, USA.

52. Y. J. Choi and Y. S. Lee, *J. Chem. Phys.*, 2003, **119**, 2014-2019.

53. W. K. Cho, Y. J. Choi and Y. S. Lee, *Mol. Phys.*, 2005, **103**, 2117-2122.

54. S. H. Vosko, L. Wilk and M. Nusair, *Can. J. Phys.*, 1980, **58**, 1200-1211.

55. C. Lee, W. Yang and R. G. Parr, *Phys. Rev. B*, 1988, **37**, 785-789.

56. A. D. Becke, *J. Chem. Phys.*, 1993, **98**, 5648-5652.

57. P. J. Stephens, F. J. Devlin, C. F. Chabalowski and M. J. Frisch, *J. Phys. Chem.*, 1994, **98**, 11623-11627.

58. T. H. Dunning, Jr., *J. Chem. Phys.*, 1989, **90**, 1007-1023.

59. R. A. Kendall, T. H. Dunning, Jr. and R. J. Harrison, *J. Chem. Phys.*, 1992, **96**, 6796-6806.

60. D. E. Woon and T. H. Dunning, Jr., *J. Chem. Phys.*, 1993, **98**, 1358-1371.

61. Y.-K. Han, C. Bae, S.-K. Son and Y. S. Lee, *J. Chem. Phys.*, 2000, **112**, 2684-2691.

62. A. S. P. Gomes and L. Visscher, *Chem. Phys. Lett.*, 2004, **399**, 1-6.

63. M. J. Frisch, G. W. Trucks, H. B. Schlegel, G. E. Scuseria, M. A. Robb, J. R. Cheeseman, J. A. Montgomery Jr., T. Vreven, K. N. Kudin, J. C. Burant, J. M. Millam, S. S. Iyengar, J. Tomasi, V. Barone, B. Mennucci, M. Cossi, G. Scalmani, N. Rega, G. A. Petersson, H. Nakatsuji, M. Hada, M. Ehara, K. Toyota, R. Fukuda, J. Hasegawa, M. Ishida, T. Nakajima, Y. Honda, O. Kitao, H. Nakai, M. Klene, X. Li, J. E. Knox, H. P. Hratchian, J. B. Cross, V. Bakken, C. Adamo, J. Jaramillo, R. Gomperts, R. E. Stratmann, O. Yazyev, A. J. Austin, R. Cammi, C. Pomelli, J. W. Ochterski, P. Y. Ayala, K. Morokuma, G. A. Voth, P. Salvador, J. J. Dannenberg, V. G. Zakrzewski, S. Dapprich, A. D. Daniels, M. C. Strain, O. Farkas, D. K. Malick, A. D. Rabuck, K. Raghavachari, J. B. Foresman, J. V. Ortiz, Q. Cui, A. G. Baboul, S. Clifford, J. Cioslowski, B. B. Stefanov, G. Liu, A. Liashenko, P. Piskorz, I. Komaromi, R. L. Martin, D. J. Fox, T. Keith, M. A. Al-Laham, C. Y. Peng, A. Nanayakkara, M. Challacombe, P. M. W. Gill, B. Johnson, W. Chen, M. W. Wong, C. Gonzalez and P. J. A., *Gaussian 03, Revision C.02*, (2004) Gaussian Inc., Wallingford CT.

64. V. Barone and M. Cossi, *J. Phys. Chem. A*, 1998, **102**, 1995-2001.

65. M. Cossi, N. Rega, G. Scalmani and V. Barone, *J. Comput. Chem.*, 2003, **24**, 669-681.

66. Y. Takano and K. N. Houk, *J. Chem. Theory Comput.*, 2005, **1**, 71-78.

67. V. Barone, M. Cossi and J. Tomasi, *J. Chem. Phys.*, 1997, **107**, 3210-3221.

68. C. P. Kelly, C. J. Cramer and D. G. Truhlar, *J. Phys. Chem. B*, 2007, **111**, 408-422.

69. C. J. Cramer, *Essentials of Computational Chemistry : Theories and Models*, 2nd edn., J. Wiley and Sons, Chichester, 2004.

70. I. Dreyer, R. Dreyer, V. A. Chalkin and M. Milanov, *Radiochem. Radioanal. Lett.*, 1979, **40**, 145-153.